PRL **95,** 216602 (2005) PHYSICAL REVIEW LETTERS week ending 18 NOVEMBER 2005

Electrical Switching in Metallic Carbon Nanotubes

Young-Woo Son,[1,2] Jisoon Ihm,[2,3] Marvin L. Cohen,[1] Steven G. Louie,[1] and Hyoung Joon Choi[4,*]
[1]*Department of Physics, University of California at Berkeley*
and Materials Sciences Division at Lawrence Berkeley National Laboratory, Berkeley, California 94720, USA
[2]*School of Physics, Seoul National University, Seoul 151-742, Korea*
[3]*Department of Physics, Sungkyunkwan University, Suwon 440-746, Korea*
[4]*School of Computational Sciences, Korea Institute for Advanced Study, Seoul 130-722, Korea,*
and Institute of Physics and Applied Physics, Yonsei University, Seoul 120-749, Korea
(Received 26 April 2005; published 17 November 2005)

We present first-principles calculations of quantum transport which show that the resistance of metallic carbon nanotubes can be changed dramatically with homogeneous transverse electric fields if the nanotubes have impurities or defects. The change of the resistance is predicted to range over more than 2 orders of magnitude with experimentally attainable electric fields. This novel property has its origin that backscattering of conduction electrons by impurities or defects in the nanotubes is strongly dependent on the strength and/or direction of the applied electric fields. We expect this property to open a path to new device applications of metallic carbon nanotubes.

DOI: 10.1103/PhysRevLett.95.216602 PACS numbers: 72.80.Rj, 73.63.Fg, 81.05.Tp

Are single-walled carbon nanotubes (SWNTs) suitable for future nanoelectronic device applications? The answer depends on whether the electrical properties of carbon nanotubes are changeable by applied gate voltages or electric fields [1]. Carbon nanotubes are either semiconducting or metallic, depending on their atomic geometry (diameter and chirality). Semiconducting carbon nanotubes are well suited for nanoelectronic device applications [2–5] because their electrical resistance is controllable by the gate voltage just as in silicon-based field-effect transistors. On the other hand, metallic nanotubes reportedly have electrical resistances which are not sensitive to the gate voltage or homogeneous transverse electric fields [6–9], and this insensitivity has discouraged device applications of the metallic ones. The previous reports on metallic nanotubes, however, are limited to clean ones with electric fields [8–12] or to defective ones without electric fields [13–16] even though impurities or structural defects under the transverse electric field may produce exotic effects because of the low dimensionality of the nanotubes.

A clean armchair-type SWNT is metallic with two linear bands intersecting at the Fermi energy (E_F) regardless of its diameter [17] [Fig. 1(a)]. The tube's electrical resistance is determined by its electronic structure.

A clean metallic SWNT should have an electrical resistance of 6.5 kΩ in two-probe measurements with perfect electrical contacts [17,18]. This results from the resistance quantum, 12.9 kΩ [19,20] (which is $h/2e^2$, with h Planck's constant and e the charge of an electron) divided by the number of bands at E_F. The resistance of a clean metallic carbon nanotube is insensitive to a homogeneous transverse (i.e., perpendicular to the tubular axis) electric field. Although the applied electric field polarizes the nanotube along the field direction [21] and the band dispersion is modified near E_F [Fermi velocities are slightly decreased as shown in Fig. 1(b)], electric fields of moderate strength do not change the number of bands at E_F [8–11], which is the only material parameter that determines the resistance of a clean one-dimensional sample. Contrary to the clean tube case, however, a defective metallic carbon nanotube, as will be shown in this Letter, will have an electrical resistance which is very sensitive to transverse electric fields, and this property may be exploited for switching device applications.

Our study of the resistance of defective metallic SWNTs in transverse electric fields (Fig. 2) is based on first-principles calculations [22]. We introduce either impurities or structural defects into metallic nanotubes and describe their atomic and electronic structures using norm-conserving pseudopotentials [23] with Kleinman-Bylander's nonlocal projectors [24] and the local density approximation for the exchange-correlation potential. The wave function is expanded with a single zeta basis set [22]

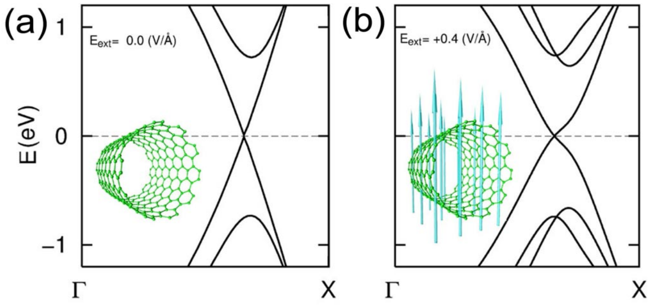

FIG. 1 (color online). Electronic structure of a clean SWNT with and without a transverse electric field ($E_{\rm ext}$). The Fermi level is set to zero in all figures. (a) Band structure near the Fermi level of a clean (10, 10) SWNT with $E_{\rm ext} = 0$. The inset is the atomic structure of the (10, 10) SWNT. (b) Band structure of a clean (10, 10) SWNT with $E_{\rm ext} = 0.4$ V/Å. The inset shows the nanotube and the applied electric field perpendicular to the tubular axis.

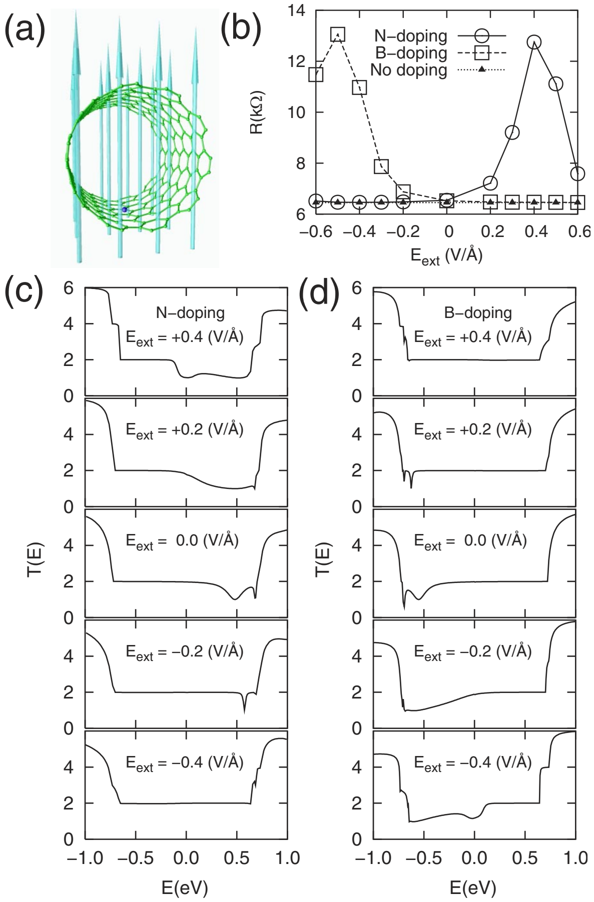

FIG. 2 (color online). Electrical resistances of single-impurity-doped SWNTs in transverse electric field E_{ext}. (a) A ball-and-stick model of a nitrogen- or boron-doped SWNT in a transverse electric field. The impurity is denoted by a darker atom. The direction of the arrows (from the impurity-doped side to the other) corresponds to $E_{\text{ext}} > 0$. (b) Calculated two-probe electrical resistances (R) of a nitrogen-doped (10, 10) SWNT, a boron-doped one, and a clean one. Transmission spectra $T(E)$ of (c) a nitrogen-doped and (d) a boron-doped (10, 10) SWNT in various transverse electric fields.

to produce the similar relaxed geometric configurations with the defect and the electronic structures compared with the result using plane-wave basis set [13]. A periodic sawtooth-type potential perpendicular to the direction of the tube axis is used to simulate the applied transverse electric field in a supercell having 420 carbon atoms for the (10, 10) nanotube and 576 atoms for the (18, 0) tube, respectively, and such a potential is homogeneous along the tube axis as shown in the inset of Fig. 1(b). By calculating the scattering wave functions of electrons around the defects, we obtain the quantum-mechanical probability for an electron near E_F to transmit through the defects [25,26]. The two-probe resistance of the sample is inversely proportional to the obtained transmission probability as well as the number of bands [27]. Our calculational results show that the resistance of defective metallic SWNTs is very sensitive to the strength and/or direction of the applied transverse electric field (Figs. 2–4).

Impurities or structural defects in metallic nanotubes produce quasibound states which backscatter conducting electrons resonantly near the quasibound-state energies. In the case of a nitrogen- and a boron-doped (10, 10) nanotube [Fig. 2(a)], the electrical resistance shows maximum values at the electric field of 0.4 and -0.5 V/Å, respectively [Fig. 2(b)]. Without electric fields, the nitrogen (boron) impurity produces resonant backscattering dips in the transmission associated with donorlike (acceptorlike) quasibound states above (below) E_F as shown in the middle panels (denoted by $E_{\text{ext}} = 0.0$ V/Å) of Figs. 2(c) and 2(d) [13].

When transverse electric fields are applied, the field-induced change of the screened electrostatic potential near the impurity sites changes the quasibound-state energies and thereby the resonant backscattering and the resistance of the nanotubes [Figs. 2(c) and 2(d)]. With an electric field, the dips move in the same direction in energy for both the nitrogen and the boron impurity. The shapes of the dips are distorted when the dips approach the Fermi level or subband edges. The maximum resistances are about twice the zero-field resistance because, at the corresponding electric fields, half of the conducting electrons at E_F are backscattered by the impurities. Since the resonant backscatterings are shifted energetically by the field-induced potential change at a defect site, the effect of the electric field scales as $|E_{\text{ext}}|\cos\theta$ approximately when the electric field (E_{ext}) has an angle θ with the normal direction of the tubular surface at the defect site. So, the effect is maximized if $\theta = 0$ as shown in Fig. 1(a). We have also examined, by first-principles calculations, electrical properties of single-impurity-doped semimetallic $(3n, 0)$ carbon nanotubes which have very small energy gaps due to the curvature effect [28]. Our calculation results show that, with transverse electric fields, the resistance of a doped (18, 0) SWNT, which is measured at either the conduction or the valence band edge, has almost the same tunable behavior (not shown here).

By adding up the effects of the nitrogen and the boron impurity in a single nanotube, we can produce a much larger variation of the resistance so that with nitrogen and boron codoping, a metallic carbon nanotube shows an ‘‘on-to-off’’ switching behavior as a function of the applied electric field [Fig. 3(b)]. When two carbon atoms on opposite sides of a (10, 10) nanotube are replaced by a nitrogen and a boron atom [Fig. 3(a)], the resistance of the nanotube is slightly (3%) increased when no transverse electric field is present [Fig. 3(b)]. It remains in the low-resistive ‘‘on state’’ (6.7 kΩ). When an electric field of 0.4 V/Å pointing from the nitrogen-doped side to the boron-doped side [Fig. 3(a)] is applied, the resistance of the nanotube increases to 221 kΩ, switching to a high-resistive ‘‘off state’’ [Fig. 3(b)]. With further increase in the strength of the electric field, the resistance decreases back to 20 kΩ.

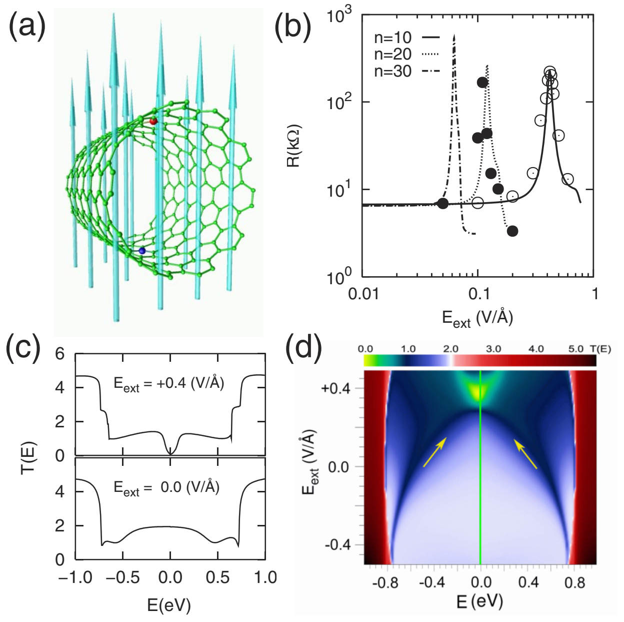

FIG. 3 (color online). Electrical resistance of nitrogen and boron codoped SWNTs in transverse electric field E_{ext}. (a) A schematic diagram of a nitrogen (blue or dark grey dot) and boron (red or grey dot) codoped SWNT in a transverse electric field. The direction of the arrows corresponds to $E_{\mathrm{ext}} > 0$. (b) Calculated two-probe electrical resistances (R) of nitrogen and boron codoped (n, n) SWNTs ($n = 10, 20, 30$). Open and solid circles are results from *ab initio* calculations for (10, 10) and (20, 20) SWNTs, respectively, and lines are results from tight-binding approximations. (c) Transmission spectra $T(E)$ of the nitrogen and boron codoped (10, 10) SWNT in electric fields of 0.0 and 0.4 V/Å. (d) Color-scale plot of transmission spectra $T(E)$ as a function of energy E and electric field E_{ext} for the nitrogen and boron codoped (10, 10) SWNT. The color-scale bar is placed on top of the plot.

When the direction of the electric field is reversed, the doped nanotube remains in the low-resistive on state (less than 10 kΩ) at all values of field strength.

The high-resistive off state of the N and B codoped metallic nanotubes originates from the impurity-induced resonant backscatterings which reflect most of the conducting electrons at E_F. With no electric field, resonant scatterings due to the N and the B impurity occur above and below E_F, respectively, reflecting half of the conducting electrons at their respective resonant energies [Fig. 3(c)]. With nonzero E_{ext}, the field-induced potential shifts are of the opposite sign near the two impurities since the two impurities are placed at opposite sides of the tube. This makes resonant backscatterings by the two impurities move in opposite directions in energy (toward E_F), and, with a specific E_{ext}, they meet at E_F, causing almost complete reflection of the conducting electrons [Fig. 3(c)] and thereby the large increase of the resistance. In Fig. 3(d), it is shown that, with electric fields, resonant backscattering dips (dark blue or dark grey) associated with the boron and the nitrogen impurity move in opposite directions (denoted by yellow arrows) in energy because they are located on opposite sides of the nanotube. With $E_{\mathrm{ext}} \simeq 0.4$ V/Å in Fig. 3(d), the two dips merge, making transmission almost zero (yellow region) at E_F (green vertical line).

The relative position of the boron and nitrogen impurities on the tubular surface affects the magnitude of the maximum resistance at the off state. Let z be the distance of the two impurities along the tubular axis and ϕ be their polar-angle difference. When $\phi = 180°$ and $z = (3n \pm 1) \times L$ for integral n [as shown in Fig. 3(a)], the maximum resistance at the off state is about 221 kΩ. Here, L is the unit-cell length of the armchair-type nanotube. If $\phi = 0°$ and $z = 3n \times L$, only one conduction channel is blocked at the maximal resistance condition, resulting in the maximal resistance of about 13 kΩ. These features are coherent effects of the two impurity scatterings, which occurs if the two impurities are closer than the phase coherence length of the electrons.

In a larger-diameter SWNT, the electrical switching is possible with a weaker electric field. First-principles calculations are preformed for different diameter defective tubes up to the (20, 20) carbon nanotubes, and we adopt tight-binding calculations to even larger-diameter nanotubes such as (30, 30) and (40, 40) tubes [Fig. 3(b)]. The tight-binding approximation here adopts the standard one π-electron model with the nearest-neighbor hopping interaction [29]. A nitrogen (boron) impurity is represented by an attractive (repulsive) Gaussian on-site potential and the applied electric field is expressed with the on-site-energy variation screened with a dielectric constant. Parameters for impurity potentials and the dielectric constant are fit to reproduce our first-principles calculations of the doped (10, 10) nanotubes. The required field strength to maximum resistance is found to be approximately inversely proportional to the square of the diameter of the nanotube. This scaling is due to the product of two effects: the field-induced potential drop across the tube diameter increases linearly and the subband energy interval decreases linearly with the increase of the diameter of the nanotubes [30]. For example, the off state for a nitrogen-boron codoped (30, 30) nanotube can be reached by a field of 0.06 V/Å [Fig. 3(b)]. Thus, the switching behavior will be more easily achieved in experiments with larger-diameter nanotubes.

An "off-to-on" switching behavior occurs when considering a carbon nanotube with a vacancy. A recent observation on graphene layers and SWNTs [31] by transmission electron microscopy reveals stable intrinsic vacancy defects under strong electric field. When four adjacent carbon atoms are removed in a (10, 10) SWNT [shown in the inset of Fig. 4(a)], for example, the nanotube is in a high-resistive off state with no electric field. Resonant backscatterings are at E_F and the resistance is 1.2 MΩ [Fig. 4(a)]. As a transverse electric field is applied, regard-

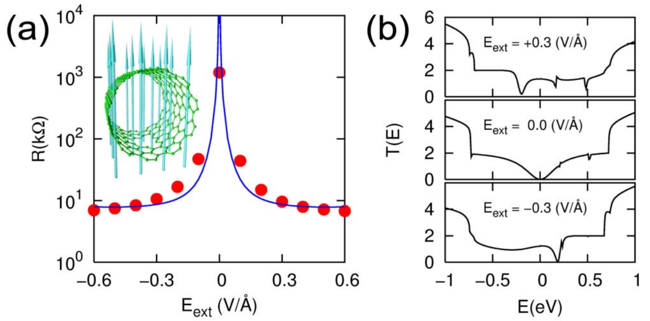

FIG. 4 (color online). (a) Calculated two-probe resistance of a (10, 10) SWNT with a vacancy in transverse electric fields ($E_{\rm ext}$). Solid circles result from *ab initio* calculations, while the solid line is from a tight-binding approximation. The direction of the electric field in the inset represents $E_{\rm ext} > 0$. (b) Transmission spectra [$T(E)$] of the (10, 10) SWNT with the vacancy as a function of energy (E). From the top to the bottom panel, the applied fields are +0.3, 0.0, and −0.3 V/Å, respectively.

less of the sign of the field, the resonant backscatterings move away from E_F [Fig. 4(b)] and the nanotube switches to a low-resistive on state having the resistance less than 20 kΩ for $|E_{\rm ext}| \geq 0.12$ V/Å (less than 100 kΩ for $|E_{\rm ext}| \geq 0.04$ V/Å) [32].

In summary, we have shown theoretically that the resistance of SWNTs is tunable up to 3 orders of magnitude by both defects and transverse electric fields, even if the SWNTs are metallic. Such a result may open a new way to make electronic devices by exploiting the variation of the resistance in metallic and semiconducting nanotubes simultaneously as a function of the electric field. The possible randomness of the size of defects and those distributions and the stability of defects under the electric fields will require future work [33]. We anticipate that this interesting property of the defective metallic SWNTs can be tested by suitable experimental setup, e.g., isolated nanotube in a nanoelectromechanical system [34] or in a split-gate configuration [35].

Y.-W. S., M. L. C., and S. G. L. were supported by NSF Grant No. DMR04-39768 and by the Director, Office of Science, Office of Basic Energy under Contract No. DE-AC03-76SF00098. J. I. was supported by the SRC program (Center for Nanotubes and Nanostructured Composites) of MOST/KOSEF. Computational resources have been provided by the KISTI, NSF at the NPACI, and DOE at the NERSC.

---

*Electronic address: h.j.choi@yonsei.ac.kr

[1] P. L. McEuen, M. S. Fuhrer, and H. Park, IEEE Trans. Nanotechnol. **1**, 78 (2002).
[2] S. J. Tans, A. R. M. Verschueren, and C. Dekker, Nature (London) **393**, 49 (1998).
[3] H. T. Soh *et al.*, Appl. Phys. Lett. **75**, 627 (1999).
[4] R. Martel *et al.*, Phys. Rev. Lett. **87**, 256805 (2001).
[5] A. Javey *et al.*, Nature (London) **424**, 654 (2003).
[6] P. L. McEuen *et al.*, Phys. Rev. Lett. **83**, 5098 (1999).
[7] J. Nygård *et al.*, Appl. Phys. A **69**, 297 (1999).
[8] J. O'Keeffe, C. Wei, and K. Cho, Appl. Phys. Lett. **80**, 676 (2002).
[9] Y. Li, S. V. Rotkin, and U. Ravaioli, Nano Lett. **3**, 183 (2003).
[10] D. S. Novikov and L. S. Levitov, cond-mat/0204499.
[11] Y.-H. Kim and K. J. Chang, Phys. Rev. B **64**, 153404 (2001).
[12] S. Barraza-Lopez *et al.*, Europhys. Lett. **69**, 1003 (2005).
[13] H. J. Choi *et al.*, Phys. Rev. Lett. **84**, 2917 (2000).
[14] T. Kostyrko, M. Bartkowiak, and G. D. Mahan, Phys. Rev. B **59**, 3241 (1999).
[15] T. Ando, J. Phys. Soc. Jpn. **74**, 777 (2005).
[16] J. Zhao and R. Xie, J. Nanosci. Nanotech. **3**, 459 (2003).
[17] R. Saito, G. Dresselhaus, and M. S. Dresselhaus, *Physical Properties of Carbon Nanotubes* (Imperial College Press, London, 1998).
[18] S. Frank *et al.*, Science **280**, 1744 (1998).
[19] R. Landauer, Philos. Mag. **21**, 863 (1970).
[20] D. S. Fisher and P. A. Lee, Phys. Rev. B **23**, R6851 (1981).
[21] L. X. Benedict, S. G. Louie, and M. L. Cohen, Phys. Rev. B **52**, 8541 (1995).
[22] J. M. Soler *et al.*, J. Phys. Condens. Matter **14**, 2745 (2002).
[23] N. Troullier and J. L. Martins, Phys. Rev. B **43**, 1993 (1991).
[24] L. Kleinman and D. M. Bylander, Phys. Rev. Lett. **48**, 1425 (1982).
[25] H. J. Choi, M. L. Cohen, and S. G. Louie (to be published).
[26] Y.-G. Yoon *et al.*, Phys. Rev. Lett. **86**, 688 (2001).
[27] S. Datta, *Electronic Transport in Mesoscopic Systems* (Cambridge University Press, Cambridge, England, 1995).
[28] M. Ouyang *et al.*, Science **292**, 702 (2001).
[29] R. Saito *et al.*, Phys. Rev. B **46**, 1804 (1992).
[30] The approximate scaling behavior can be shown from the Lippmann-Schwinger formalism. The scattered wave $|\psi\rangle$ by the impurity is $|\psi\rangle = |\varphi\rangle + \hat{G}\hat{V}_N|\psi\rangle$ with the incoming state $|\varphi\rangle$, the Green function $\hat{G}$, and the nitrogen impurity potential $\hat{V}_N$. The applied $E_{\rm ext}$ changes $\hat{G}$ to the first order by $\delta\hat{G} = \sum_n \frac{|\varphi_n\rangle\langle\delta\varphi_n| + |\delta\varphi_n\rangle\langle\varphi_n|}{E - E_n}$, which scales as $|\mathbf{E}_{\rm ext}|r^2$ because $E - E_n \propto 1/r$ and $|\delta\varphi_n\rangle\langle\varphi_n| \simeq \sum_{m=n\pm1} \times \frac{\langle\varphi_n|\mathbf{E}_{\rm ext}\cdot\mathbf{z}|\varphi_m\rangle}{E_n - E_m}|\varphi_m\rangle\langle\varphi_n| \propto \frac{|\mathbf{E}_{\rm ext}|r(1/\sqrt{r})^2}{1/r} = |\mathbf{E}_{\rm ext}|r$. Here, r is the radius of a SWNT, and we used $E_n - E_m \propto 1/r$ [17] and the selection rule ($m - n = \pm1$) of the subband mixing [11].
[31] A. Hashimoto *et al.*, Nature (London) **430**, 870 (2004).
[32] Vacancy defects with hydrogen passivations to σ bonds are found to provide a single or multiple quasibound states from π orbitals around E_F depending on the number of removed atoms. The detailed calculations on various vacancy defects will be published elsewhere.
[33] Preliminary first-principles calculations were performed to show similar switching behaviors in (10, 10) SWNT doped with multiple (two and three) nitrogens, two boron and two nitrogen, and three boron and one nitrogen substitutional impurities in various configurations.
[34] A. M. Fennimore *et al.*, Nature (London) **424**, 408 (2003).
[35] S.-B. Lee *et al.*, J. Nanosci. Nanotech. **3**, 325 (2003).